Progress In Electromagnetics Research C, Vol. 21, 99–111, 2011

MICROSTRIP BANDPASS FILTERS USING DUAL-MODE RESONATORS WITH INTERNAL COUPLED LINES

C. Hua, C. Chen, C. Miao, and W. Wu

Ministerial Key Laboratory of JGMT
Nanjing University of Science and Technology, Nanjing 210094, China

Abstract—This paper presents a new dual-mode stub-loaded resonator, which consists of a microstrip resonator with internal coupled lines and an open-circuited stub. Based on the odd- and even-mode equivalent circuits, the resonant characteristics of the proposed microstrip resonator are investigated. It is found that the fundamental even-mode resonant frequency of the proposed resonator can be flexibly controlled while the fundamental odd-mode resonant frequency remains unaffected. Then, based on the proposed resonator, three compact dual-mode bandpass filters, namely filer A, filter B and filter C, are designed, fabricated and measured to validate the design concept. Filters A and B demonstrate opposite asymmetric responses with two transmission poles in the passband and a transmission zero in the stopband. Filter C has three transmission poles in the passband and two transmission zeros respectively in the lower and upper stopbands to enhance selectivity. The experimental results show excellent agreement with the theoretical simulation results.

1. INTRODUCTION

Generally speaking, bandpass filters can be designed using single- or dual-mode resonators. Dual-mode resonators are attractive because each dual-mode resonator can be used as a doubly tunable resonant circuit. Therefore the number of resonators in a filter can be reduced by half, thus resulting in a compact configuration. Various kinds of dual-mode resonators have been investigated, including the circular ring [1], square loop [2], and triangular patch [3]. Meanwhile, several new types

Received 10 March 2011, Accepted 14 April 2011, Scheduled 19 April 2011
Corresponding author: Changzhou Hua (huachangzhou@126.com).

of dual-mode resonators [4–9] have been reported for filter applications recently. Practically, some special applications of bandpass filters may require high selectivity on only one side of the pass band, but less or none on the other side. In such cases, using filters with asymmetric frequency responses would be desirable [10–12].

This paper presents a dual-mode stub-loaded resonator with internal coupled lines. The properties of the proposed resonator are analyzed theoretically and confirmed by full-wave simulations. The fundamental even-mode resonant frequency of the proposed resonator can be flexibly controlled while the fundamental odd-mode resonant frequency is unaffected. It is also found that there is a finite-frequency transmission zero inherently through the stopband. Then, based on the proposed resonator, three compact dual-mode bandpass filters, namely filer A, filter B and filter C, are designed, fabricated and measured to validate the design concept. Filters A and B are designed with two transmission poles in the passband and demonstrated with opposite asymmetric responses which result from different locations of the transmission zero. Filter A exhibits a nice asymmetric frequency response with a finite-frequency transmission zero above passband, thus leading to a good upper stopband rejection. Filter B also exhibits a nice asymmetric frequency response but with a finite-frequency transmission zero below passband, thus resulting in a good lower stopband rejection. Filter C is designed with three transmission poles in the passband and two finite-frequency transmission zeros respectively in the lower and upper stopbands to enhance selectivity. All the presented filters are fabricated on a Rogers4003 substrate with a dielectric constant of 3.38, a loss tangent of 0.0027, and a thickness of 0.813 mm.

2. DUAL-MODE RESONATOR

The structure of the proposed dual-mode resonator, which consists of a microstrip resonator with internal coupled lines and an open-circuited stub, is displayed in Fig. 1(a), where Y_1, θ_1, Y_3 and θ_3 denote the characteristic admittances and electric lengths of the microstrip line and open stub, respectively. Y_{odd}, Y_{even} and θ_2 indicate the odd- and even-mode characteristic admittances and electrical length of the coupled lines. Since the resonator is symmetrical in structure, the resonant condition can be analyzed by the classical method of even- and odd-mode excitation

For odd-mode excitation, there is a voltage null along the symmetrical plane A-A'. The equivalent circuit is shown in Fig. 1(b) Taking $\theta_1 = \theta_2 = \theta_3 = \theta$ for convenience, we can derive the input

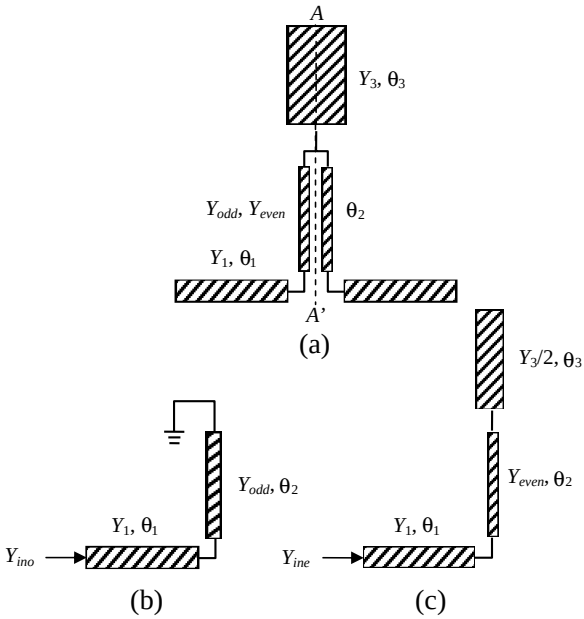

Figure 1. (a) Structure of the proposed dual-mode stub-loaded resonator, (b) odd-mode equivalent circuit, and (c) even-mode equivalent circuit.

admittance for odd-mode (Y_{ino}) as follows:

$$Y_{ino} = jY_1 \frac{Y_1 \tan^2\theta - Y_{odd}}{(Y_1 + Y_{odd})\tan\theta} \tag{1}$$

From the odd-mode resonance condition of $Y_{ino} = 0$, we obtain the following equation,

$$\tan^2\theta = K_1 = \frac{Y_{odd}}{Y_1}. \tag{2}$$

Therefore the fundamental odd-mode resonant frequency (f_{odd}) can be expressed as,

$$f_{odd} = \frac{c\tan^{-1}(\sqrt{K_1})}{2\pi L_1\sqrt{\varepsilon_{eff}}} \tag{3}$$

where c is the speed of light in free space, L_1 is the length of the microstrip line, and ε_{eff} denotes the effective dielectric constant of the substrate. It can be observed that the fundamental odd-mode resonant frequency is not affected by the open-circuited stub.

For even-mode excitation, there is no current flow through the symmetrical plane A-A'. The equivalent circuit is shown in Fig. 1(c).

When we ignore the discontinuity of the folded section, the input admittance for even-mode (Y_{ine}) can be expressed as follows:

$$Y_{ine} = jY_1 \frac{(2Y_1Y_{even} + Y_3Y_{even} + 2Y_{even}^2)\tan\theta - Y_1Y_3\tan^3\theta}{2Y_1Y_{even} - (Y_1Y_3 + Y_3Y_{even} + 2Y_{even}^2)\tan^2\theta} \tag{4}$$

From the even-mode resonance condition of $Y_{ine} = 0$, we obtain the following equation,

$$\tan^2\theta = K_2 = \frac{Y_{even}}{Y_1} + \frac{2Y_{even}^2}{Y_1Y_3} + \frac{2Y_{even}}{Y_3}. \tag{5}$$

Therefore the fundamental even-mode resonant frequency (f_{even}) can be expressed as,

$$f_{even} = \frac{c\tan^{-1}(\sqrt{K_2})}{2\pi L_1\sqrt{\varepsilon_{eff}}} \tag{6}$$

From the analysis above, we can conclude that the resonance conditions of the proposed resonator are determined by K_1, K_2 and θ. If $K_1 = K_2$, both fundamental resonant frequencies are exactly the same. If $K_1 < K_2$, then the resonator can generate a higher f_{even} than f_{odd}. And if $K_1 > K_2$, the resonator will make f_{even} lower than f_{odd}. In our investigation, we only change the value of Y_3, while keeping all other parameters constant. The structural parameters of the resonator are listed as follows: $Y_1 = 0.0125\,\mathrm{S}$, $Y_{odd} = 0.02\,\mathrm{S}$, $Y_{even} = 0.01\,\mathrm{S}$, $\theta_1 = \theta_2 = \theta_3 = \theta = 0^\circ$ at 2 GHz. To observe the mode splitting, full-wave simulations have been carried out by using ADS. As shown in Fig. 2, two coupling capacitors of 0.05 pF are used for a loose coupling. By tuning the value of Y_3, different frequency responses can be achieved. As Y_3 increases, K_2 decreases while K_1 is constant. The simulated responses are shown in Fig. 3. When K_2

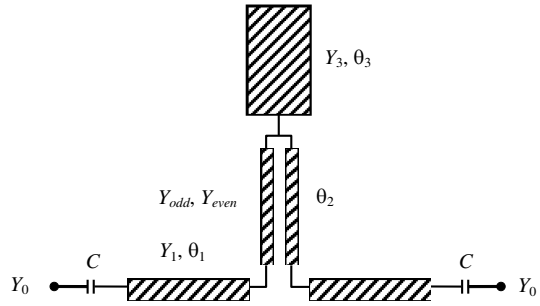

Figure 2. Proposed resonator with coupling capacitor C for a loose coupling.

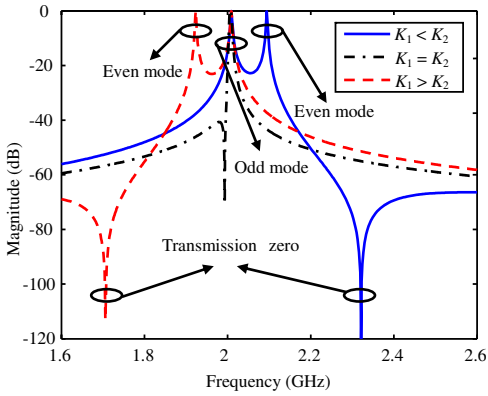

Figure 3. Modal resonant characteristic of the proposed resonator.

is larger than K_1, the fundamental even-mode resonant frequency is beyond the fundamental odd-mode resonant frequency. When K_1 is equal to K_2, the fundamental resonant frequencies of the two modes are the same. And when K_2 is smaller than K_1, the fundamental even-mode resonant frequency is below the fundamental odd-mode resonant frequency. As a result, the fundamental even-mode resonant frequency of the proposed resonator can be flexibly controlled while the fundamental odd-mode resonant frequency is unaffected.

Besides, it can be seen from Fig. 3 that there is a transmission zero inherently through the stopband. And the transmission-zero frequency of the resonator can also be tuned by varying the value of Y_3. As Y_3 increases, the transmission zero will shift from the upper to lower stopband. This unique property allows an easy design of asymmetric responses with improved selectivity below or above the passband, by just varying the width of the open-circuited stub We can predict the transmission zero from the analysis of the transmission coefficient S_{21}. Taking the source and load admittances of the circuit shown in Fig. 2 as Y_0, we can obtain the transmission coefficient S_{21} as [13],

$$S_{21} = \frac{Y_0(Y_{ino} - Y_{ine})}{(Y_0 + Y_{ine})(Y_0 + Y_{ino})}. \tag{7}$$

By letting $S_{21} = 0$, the condition of transmission zero is,

$$Y_{ino} = Y_{ine}. \tag{8}$$

From the above condition, we obtain the following equation

$$\tan^2\theta = K_3 = \frac{-b - \sqrt{b^2 - 4ac}}{2a}, \tag{9}$$

with

$$\begin{aligned} a &= Y_3 Y_{even} - Y_3 Y_{odd} + 2Y_{even}^2, \\ b &= Y_3 Y_{even} + 2Y_{even}^2 + 2Y_{even} Y_{odd} - Y_3 Y_{odd}, \\ c &= 2Y_{even} Y_{odd}. \end{aligned}$$

Therefore the transmission-zero frequency (f_{zero}) can be expressed as,

$$f_{zero} = \frac{c \tan^{-1}(\sqrt{K_3})}{2\pi L_1 \sqrt{\varepsilon_{eff}}} \tag{10}$$

Figure 4 shows the variation of the fundamental resonant frequencies and the transmission-zero frequency against different values of Y_3, with all other dimensions constant. It can be seen clearly that as Y_3 increases, the fundamental odd-mode resonant frequency is fixed, while the fundamental even-mode resonant frequency and the transmission-zero frequency keep decreasing.

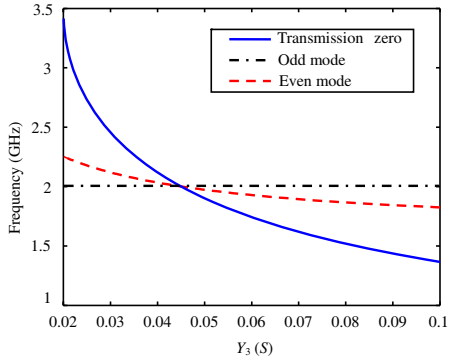

Figure 4. Variation of the fundamental resonant frequencies and the transmission-zero frequency against different values of Y_3.

Figure 5 shows the current distributions for the two modes of the proposed resonator. At the fundamental odd-mode resonant frequency, there is no current flowing on the open-circuited stub, and the open-circuited stub does not perturb the fundamental resonant current distribution. On the other hand, at the fundamental even-mode resonant frequency, there is current flowing on the open-circuited stub, which changes the current distribution path, thus changing the resonant frequency

As we know, coupling coefficient of resonator plays a key role in determining the bandwidth of a filter. The inter-stage coupling coefficient of a dual-mode filter corresponds to the coupling between the two modes of the dual-mode resonator. An approximate method based

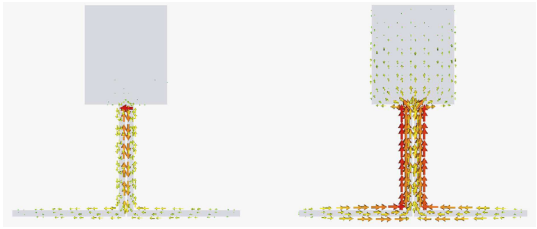

Figure 5. Simulated current distributions for the two modes of the proposed resonator, (a) odd mode, (b) even mode.

on the conditions of a given passband bandwidth and ripple can be used to design a dual-mode bandpass filter where capacitive coupling is adopted for input and output coupling [14]. Here we discuss the design technique for a basic dual-mode bandpass filter with only one resonator When the normalized Chebyshev low-pass filter prototype element values are $g_0 \sim g_3$, the relative bandwidth is w, and the odd- and even-mode resonance frequencies of the resonator are f_{odd} and f_{even}, respectively, the inter-stage coupling coefficient is given as follows:

$$k_{12} = \frac{w}{\sqrt{g_1 g_2}} = \frac{2\left|f_{even} - f_{odd}\right|}{f_{even} + f_{odd}}. \tag{11}$$

And the input and output coupling capacitor C_s is expressed as,

$$C_s = \frac{J_{01}}{\omega_0 \sqrt{1 - (J_{01}/G_s)^2}}, \tag{12}$$

with

$$J_{01} = \sqrt{\frac{G_s b_r w}{g_0 g_1}},$$

where the parameter ω_0 is the center angular frequency of the basic dual-mode bandpass filter, G_s is the source conductance, and b_r is the resonator slope parameter.

Based on the above design method, three basic dual-mode filters with center frequencies f_0 of 2.04 GHz and relative bandwidths of 2.0%, 4.0%, and 77% respectively, have been designed with the proposed resonator. The normalized element values of the Chebyshev low-pass filter prototype with 0.01 dB ripple can be obtained from [15] as, $g_0 = 1$, $g_1 = 0.4488$, $g_2 = 0.4077$, $g_3 = 1.1007$. Subsequently the design parameters are summarized in Table 1 while the simulated results are shown in Fig. 6.

Table 1. Dual-mode filter design parameters.

Filter Type	I	II	III
Center frequency f_0	2.04 GHz		
Relative Bandwidth w	2.0%	4.0%	7.7%
Coupling Coefficient k_{12}	0.0468	0.0935	0.180
Coupling Capacitance C_s	0.17 pF	0.24 pF	0.37 pF

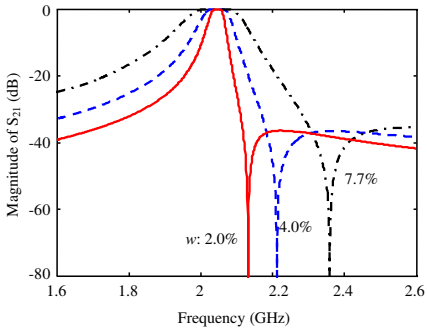

Figure 6. Simulated responses of the basic dual-mode filters.

3. FILTER DESIGN

3.1. Two-pole Filter

To validate the design concept, two two-pole filters using the proposed resonator are fabricated and measured, namely filer A and filter B. The two filters demonstrate opposite asymmetric responses with two transmission poles in the passband and a transmission zero in the stopband. Fig. 7 illustrates the configuration of the two-pole filter. It consists of a resonator and two stepped-impedance feed lines which feed the proposed resonator with tight coupling.

Figure 8 shows the photograph of filter A, of which the dimensions are listed as follows: $W_0 = 1.81\,\text{mm}$, $W_1 = 0.76\,\text{mm}$, $W_2 = 0.81\,\text{mm}$, $W_3 = 2.8\,\text{mm}$, $L_0 = 10\,\text{mm}$, $L_1 = 12.9\,\text{mm}$, $L_2 = 13.1\,\text{mm}$, $L_3 = 12.27\,\text{mm}$, $L_4 = 14\,\text{mm}$, $S_1 = 0.12\,\text{mm}$, $S_2 = 0.21\,\text{mm}$, $d = 3.62\,\text{mm}$. Fig. 9 illustrates the simulated and measured results of filter A. Frequency responses are simulated by CST-MWS and measured by Agilent 8722ES network analyzer. As shown in Fig. 9, the filter has an asymmetrical frequency response with two transmission poles in the passband and a transmission zero in the upper stopband. Owing to the fabrication tolerance, the measured center frequency (f_0) of

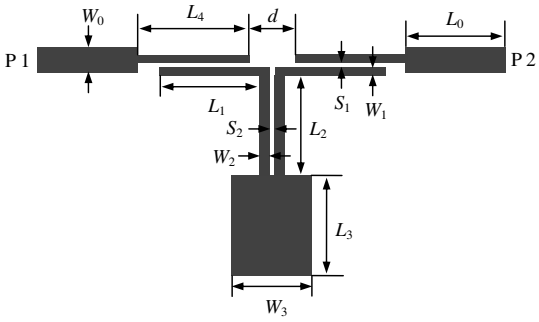

Figure 7. Configuration of the two-pole filter.

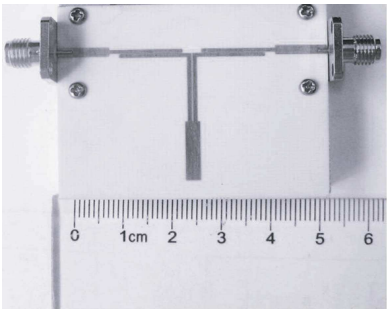

Figure 8. Photograph of filter A.

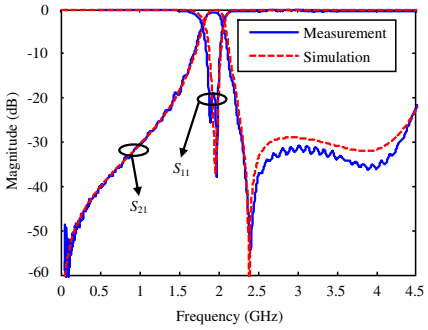

Figure 9. Frequency responses of filter A.

1.95 GHz is slightly lower than the simulated 1.96 GHz. The filter has an insertion loss of better than 0.8 dB and a return loss nearly of 19 dB at 1.95 GHz. The fractional 3-dB bandwidth of this filter is 13.1%, and the transmission zero at 2.40 GHz has an attenuation level of 53 dB. Besides, it can be seen that the first spurious response of the filter does not occur at $2f_0$, but at a higher frequency, thus accounting for the wide upper stopband. The rejection is better than 30 dB from 2.3 to 4.3 GHz.

The results shown in Fig. 4 indicate that the transmission-zero frequency can be controlled by Y_3. Hence, the dimension of W_3 is tuned in order to achieve an asymmetrical frequency response with a transmission zero in the lower stopband. Fig. 10 shows the photograph of filter B. All the dimensions of filter B are the same as those of filter A except the width of the open-circuited stub. For filter B, W_3 is chosen to be 9.5 mm. As shown in Fig. 11, the filter has an asymmetrical frequency response with two transmission poles in the passband and

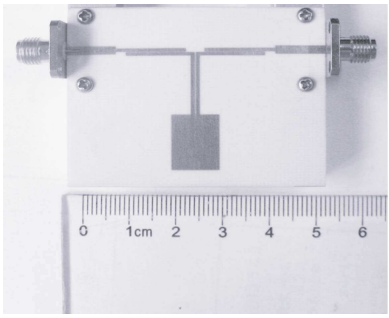

Figure 10. Photograph of filter B.

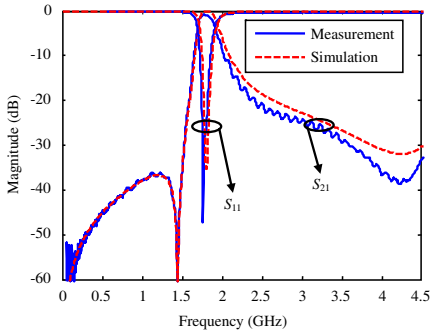

Figure 11. Frequency responses of filter B.

a transmission zero in the lower stopband. Owing to the fabrication tolerance, the measured center frequency (f_0) of 1.80 GHz is slightly lower than the simulated 1.81 GHz. The filter has an insertion loss of better than 0.85 dB and a return loss nearly of 25 dB at 1.80 GHz. The fractional 3-dB bandwidth of this filter is 12.2%, and the transmission zero at 1.45 GHz has an attenuation level of 58 dB. Besides, it can be seen that the first spurious response of the filter does not occur at $2f_0$, but at a higher frequency, which leads to a wide upper stopband.

3.2. There-pole Filter

The above two-pole filters are useful for diplexer design, as each of them has a controllable transmission zero, as well as high selectivity. However, for most applications, bandpass filters with symmetrical frequency responses are preferable. The presented two-pole filters can only provide only one transmission zero. To alleviate this difficulty, a there-pole filter is introduced.

Figure 12 illustrates the configuration of filter C. It consists of two resonators and two stepped-impedance feed lines. By properly tuning the resonant frequencies of the upper and lower resonators, filter C can provide three transmission poles in the passband and two transmission zeros respectively in the lower and upper stopbands. Fig. 13 displays the photograph of filter C. The dimensions of the filter are listed as follows: $W_0 = 1.81$ mm, $W_1 = 0.76$ mm, $W_2 = 0.81$ mm, $L_0 = 10$ mm, $L_1 = 12.9$ mm, $L_2 = 13.1$ mm, $L_3 = 12.27$ mm, $L_4 = 14$ mm, $S_1 = 0.12$ mm, $S_2 = 0.21$ mm, $d = 3.62$ mm. All dimensions of two resonators are the same except the width of the open-circuited stub. For the lower resonator, W_3 is chosen to be 2.8 mm. While for the upper one, W_3' is chosen to be 15 mm. From the previous

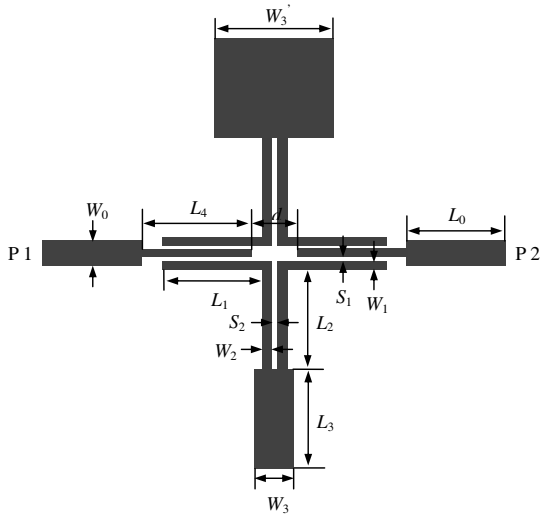

Figure 12. Configuration of filter C.

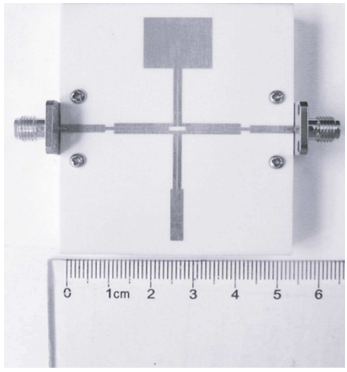

Figure 13. Photograph of filter C.

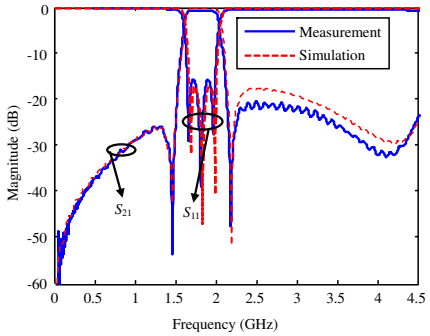

Figure 14. Frequency responses of filter C.

analysis, odd-mode resonant frequencies of these two resonators are the same, but even-mode ones are different. As a result, a three-pole filter is designed with two transmission zeros located at the two edges of the passband, as shown in Fig. 14. Owing to the fabrication tolerance, the measured center frequency of 1.84 GHz is slightly lower than the simulated 1.85 GHz. As observed from the frequency response, the filter has a 3-dB fractional bandwidth of 22.7%, an insertion loss of better than 0.7 dB, and two rejections of greater than 20 dB.

Furthermore, the two transmission zeros are at 1.46 and 2.19 GHz with 54 and 48 dB rejection, respectively. It can also be seen that, the first spurious response of the filter does not occur at $2f_0$, but at a higher frequency, thus resulting in a wide upper stopband.

4. CONCLUSION

In this paper, a dual-mode stub-loaded resonator with internal coupled lines is proposed. The properties of the resonator have been obtained by theoretical analysis and thereafter verified by simulation and experiment. The proposed resonator possesses the merit that its fundamental even-mode resonant frequency can be flexibly controlled while the fundamental odd-mode resonant frequency remains unaffected. Based on the proposed resonator, three compact dual-mode bandpass filters have been designed and manufactured. With the measured results, filter A exhibits a good insertion loss of better than 0.8 dB in the passband, and a nice asymmetric frequency response with a transmission zero in the upper stopband leading to good rejection. Similarly, the insertion loss of filter B is no more than 0.85 dB, whereas the transmission zero is located in the lower stopband. Combining the advantages of the former two filters, filter C owns an insertion loss of better than 0.7 dB inside the passband and two transmission zeros at each edge of the passband resulting in an excellent performance of frequency response. Meanwhile, the first spurious response of these three filters does not occur at $2f_0$, but at a higher frequency, thus resulting in a wide upper stopband. The measured results agree well with the simulations. Therefore, the proposed filters can be integrated in microwave circuits and systems due to their compact structures, and high performance.

REFERENCES

1. Wolff, I., "Microstrip bandpass filter using degenerate modes of a microstrip ring resonator," *Electronics Lett.*, Vol. 8, No. 12, 302–303, 1972.
2. Hong, J.-S. and M. J. Lancaster, "Bandpass characteristics of new dual-mode microstrip square loop resonators," *Electronics Lett.*, Vol. 30, No. 11, 891–892, 1995.
3. Hong, J.-S. and S. Li, "Theory and experiment of dual-mode microstrip triangular patch resonators and filters," *IEEE Trans. Microw. Theory Tech.*, Vol. 52, No. 4, 1237–1243, 2004.
4. Hong, J.-S., H. Shanman, and Y. H. Chun, "Dual-mode microstrip

open loop resonators and filters," *IEEE Trans. Microw. Theory Tech.*, Vol. 55, No. 8, 1764–1770, 2007.

5. Song, K. and Q. Xue, "Novel broadband bandpass filters using Y-shaped dual-mode microstrip resonators," *IEEE Microw. Wirel. Compon. Lett.,* Vol. 19, No. 9, 548–550, 2009.
6. Wang, Y.-X., B.-Z. Wang, and J. Wang, "A compact square loop dual-mode bandpass filter with wide stop-band," *Progress In Electromagnetics Research*, Vol. 77, 67–73, 2007.
7. Chen, Z.-X., X.-W. Dai, and C.-H. Liang, "Novel dual-mode dual-band bandpass filter using double square-loop structure," *Progress In Electromagnetics Research*, Vol. 77, 409–416, 2007.
8. Huang, C.-Y., M.-H. Weng, C.-S. Ye, and Y.-X. Xu, "A high band isolation and wide stopband diplexer using dual-mode stepped-impedance resonators," *Progress In Electromagnetics Research,* Vol. 100, 299–308, 2010.
9. Chiou, Y.-C., P.-S. Yang, J.-T. Kuo, and C.-Y. Wu, "Transmission zero design graph for dual-mode dual-band filter with periodic stepped-impedance ring resonator," *Progress In Electromagnetics Research*, Vol. 108, 23–36, 2010.
10. Hong, J.-S. and M. J. Lancaster, "Microstrip cross-coupled trisection bandpass filters with asymmetric frequency characteristics," *IEE Proc. Microw. Antennas Propag.*, Vol. 146, No. 1, 84–90, 1999.
11. Kurzrok, R. M., "General three-resonator filters in waveguide," *IEEE Trans. Microw. Theory Tech.*, Vol. 14, No. 1, 46–47, 1966.
12. Chang, C.-Y. and C.-C Chen, "A novel coupling structure suitable for cross-coupled filters with folded quarter-wave resonators," *IEEE Microw. Wirel. Compon. Lett.*, Vol. 13, No. 12, 517–519, 2003.
13. Mongia, R., I. Bahl, and P. Bhartia, *RF and Microwave Coupled-line Circuits*, Artech House, Norwood, MA, 1999.
14. Matsuo, M., H. Yabuki, and M. Makimoto, "Dual-mode stepped-impedance ring resonator for bandpass filter applications," *IEEE Trans. Microw. Theory Tech.*, Vol. 49, No. 7, 1235–1240, 2001.
15. Pozar, D. M., *Microwave Engineering*, 3rd edition, Wiley, New York, 2005.